Desalination and Water Treatment
www.deswater.com

doi:10.5004/dwt.2017.21563

94 (2017) 47–55
October

Phosphorus sorption with modified sediments from a malodorous river: kinetics, equilibrium, and thermodynamic studies

Xing Chen[a,b], Ying Lu[c], Cheng Yao[a], Xia Jiang[a,**], Wei Huang[a,*]

[a]*State Key Laboratory of Environmental Criteria and Risk Assessment, Chinese Research Academy of Environmental Sciences, Beijing, China, Tel. +86 01084913896, email: yongmouren@163.com, (X. Chen), Tel. +86 01084913896, email: yao948416159@hotmail.com (C. Yao), Tel. +86 01084913896, email: jiangxia@craes.org.cn (X. Jiang), Tel. +86 010 84913896, Fax +86 010 84913896, email: yixinghd6@163.com (W. Huang)*

[b]*College of Environment and Planning, Henan University, Kaifeng, China*

[c]*Department of Environmental Science and Engineering, Fudan University, Shanghai 200433, China, Tel. +86 021 65642948, email: luying0210@163.com (Y. Lu)*

Received 21 May 2017; Accepted 18 October 2017

ABSTRACT

Utilization of sediment resources and excessive phosphorus (P) in malodorous river caught the interest of numerous researchers. This study investigated P sorption with modified sediments from malodorous rivers through kinetics, equilibrium, and thermodynamic experiments. Results indicated that sorption rate followed the pseudo-second-order model ($R^2 > 0.93$), and when the temperature increased, the P removal efficiency of modified sediment samples increased (the highest value of 93.2%). Modified sediment materials, which are oxidation (PS-N), Na-doped (PS-Na), and oxidation-Na doped (PS-NNa), presented higher P sorption capacities than raw sediment due to changes in their surface structure. PS-NNa showed the highest sorption capacity (1.43 mg g^{-1}) in comparison other sediment materials. Data from isotherm experiments were well described by Langmuir isotherm model, and calculated thermodynamic parameters illustrated occurrence of spontaneous ($\Delta G < 0$), entropy-driven P sorption ($\Delta S > 0$) and endothermic reactions ($\Delta H > 0$).

Keywords: Phosphorus; Malodorous river; Modified sediment; Sorption; Removal

1. Introduction

In recent years, rivers in urban areas were polluted by industries, agriculture, and domestic pollutants, and rivers frequently become malodorous [1]. Malodorous rivers increase in cities of developing countries. Phosphorus (P) is an essential nutrient that limits primary production in aquatic ecology [2,3] and exists in soil, sediments, water, and organisms [4]. Excessive P caused by P fertilization practices and discharges from urban wastewater treatment plants can lead to eutrophication of rivers [5]; most malodorous rivers feature excessive P. Sediments in malodorous river act as pool of intense anthropogenic pollutant inputs and thus become major sources of pollutants after effective discharge of intercepted pollutants to river systems [1,6]. Therefore, environment-friendly methods must be developed to dispose sediments in malodorous rivers, and the methods of P removal should be explored.

Extensive researches have discussed treatment and reutilization of sediments from malodorous rivers; on-site and off-site technologies are the main methods for sediment treatment. On-site sediment treatments, such as artificial aeration [7], coagulation [8], and bioremediation [9], were studied in small scale. However, these technologies are not used in large-scale engineering applications, especially in malodorous rivers. Currently, off-site technologies of sediment treatment are commonly utilized; these technologies include dredging sediment landfills [10], dehydration after dredging [11], and sediment pyrolysis after dehydration [12]. Although dredged sediments are reutilized, products from sediment reutilization exhibit no competitiveness in comparison with products from similar fields. Sediment

*Corresponding author.

**The authors contributed equally to this article

reutilization from malodorous rivers yields low economic benefits and adequate protection.

Previous studies indicated that soils, slags, zeolite, and calcite present relatively high P removal efficiency [13,14]; alternately, some filtration materials, such as sand and burned clay coated with oxides of iron, aluminum, or manganese, can act as good P sorbents [15,16]. Our previous study indicated that modified gravel sand also exhibits high P removal efficiency [17]. However, most P materials are used in small-scale on-site systems, and difficulty arises from efficient and economical removal of high P concentrations.

Liangshui River (116°27′40.79″N, 39°49′40″E) is located in the city of Beijing, China, and measures 64.8 km in length. In recent years, city development caused increase in population around the river basin, and large amounts of pollutants were discharged into Liangshui River. Sewage treatment plants near the river lacked high capacity for sewage treatment or matching municipal drainage pipeline, and malodor in Liangshui River worsened. Thus, the present study aims to evaluate P removal efficiency using modified sediments from malodorous river and to analyze mechanism of P sorption. This study may provide new insights into P removal and sediment reutilization from malodorous rivers.

2. Materials and methods

2.1. Sediment sampling and sorption of sediment materials

The sampling information is shown in Fig. 1. Surface (10 cm) sediment samples (N = 7)were collected from Liangshui River in February 2017. Sediments were mixed and brought to the laboratory, where they were freeze-dried (for 4 days), ground, and sifted through 100-mesh sieve to obtain uniform size. Obtained raw sediment materials were designated as PS and were used in production of modified sediment materials. Afterward, 2.0 g PS were added to 100 mL 2.5 mol L^{-1}/HNO_3 solution to modify raw sediments, and resulting mixture was shaken for 24 h at room temperature (25±2°C). Modified sediments were obtained by filtration and drying and labeled as PS-N. Na-doped sediment samples were prepared by separately introducing 2.0 g PS and PS-N to 100 mL of 0.2 mol L^{-1}/NaCl solution. pH during Na loading was maintained at 2.5–3.5; then, mixtures were shaken for 24 h at room temperature (25±2°C). Modified sediment samples were then obtained by filtration and drying and named as PS-Na and PS-NNa.

2.2. Characterization of sediment materials

Total phosphorus (TP) and total nitrogen (TN) of raw sediments and water were determined using standard measurement and tests and grading extraction method. pH in raw sediments was measured in a 1:2.5 (w/w) mixture of soil with deionized water. Organic matter (OM) content was determined by loss of ignition to constant mass (4 h) at 550°C. NH_3-N concentration in water was determined using the Nessler reagent spectrophotometric method [18]. The DO and pH were measured in situ (above 30 cm of surface sediment) by using a portable multi-parameter water quality analyzer (ProPlus, YSI, USA). Surface area measurements were obtained using Micrometritics Tristar

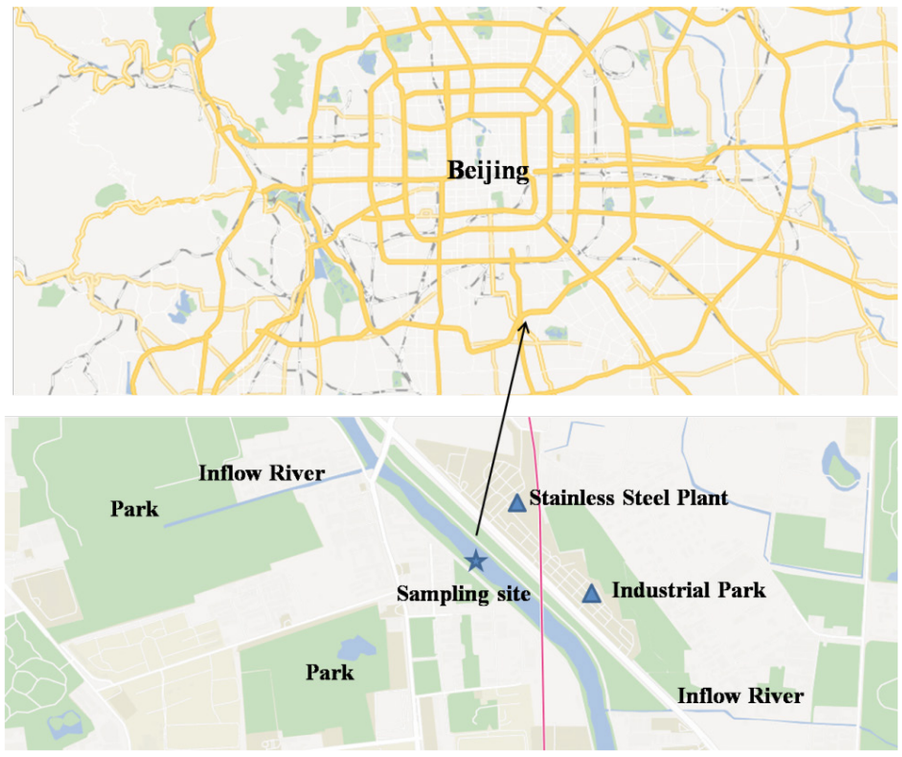

Fig. 1. Sampling site and information from Liangshui River.

3000 Surface Analyzer. Surface morphology and structure of material samples were measured using scanning electron microscopy (SEM, Philips XL 30). Oxide contents of sediment samples were measured by X-ray fluorescence analyzer (S4 Explorer, Germany). Surface functional groups were identified according to transmission infrared spectra obtained from a Fourier transform infrared (FTIR) spectrophotometer (Nicolet 6700, USA). Table 1 shows the main properties of sediments and water in Liangshui River, and Table 2 shows the characteristics of four sediment materials.

2.3. Experiment design

2.3.1. Kinetics sorption experiments

Phosphorus sorption kinetics was examined in a solution with initial phosphorus concentrations of 10 mg L^{-1} at different temperatures (15, 25 and 35°C). Sediment materials (1 g) were added into a series of 100-mL conical flasks mixed with 50 mL P solution which was prepared with KH_2PO_4. The conical flasks were shaken (220 rpm) in a constant temperature of 15°C, 25°C, and 35°C individually. At 13 different time intervals (0, 1, 2, 4, 8, 10, 20, 40, 60, 120, 240, 360, and 480 min), suspensions were obtained from each flask, and then centrifuged, filtered (0.45 um), analyzed for P concentration. The experiments were conducted in triplicate, and the sediment materials (1 g) to solution (50 mL) ratio was assumed constant throughout the incubation period.

2.3.2. Sorption isotherm experiments

The sorption isotherm of P by sediment materials were obtained by using batch experiments. The sediment materials (PS, PS-Na, PS-N, and PS-NNa) of 1 g were added to a series of 100-mL conical flasks containing 50 mL P solution at different concentrations (0, 1, 2, 5, 10, 20, and 50 mg L^{-1} as KH_2PO_4). The conical flasks were continuously agitated on a shaker with a speed of 220 rpm and different temperatures of 15°C, 25°C, and 35°C for a 48 h. The suspensions were centrifuged, filtered (0.45 um), and analyzed to determine P. The experiments were conducted in triplicate, and the sediment materials (1 g) to solution (50 mL) ratio was assumed constant throughout the incubation period.

2.3.3. Thermodynamic parameters

Sediment materials (1 g) were added into 50 mL P solution with various initial concentrations (0, 1, 2, 5, 10, 20, and 50 mg L^{-1} as KH_2PO_4) at three different temperature: 15°C, 25°C, and 35°C. Batch samples were agitated in a temperature-controlled shaker for 8 h. The thermodynamic parameters of P sorption, such as enthalpy (ΔH), Gibbs energy (ΔG), and entropy (ΔS), were determined by fitting linear equations to the thermodynamic data obtained under different concentrations.

2.4. Data analysis

P uptake of different sediment materials at each time (mg g^{-1}) were calculated as follows:

$$Q_t = \left(C_0 - C_t\right)\frac{V}{W} \tag{1}$$

P removal efficiency η (%) was calculated by the following equation:

$$\eta\% = \frac{(C_0 - C_t)}{C_0} \times 100\% \tag{2}$$

where C_0 (mg L^{-1}) refers to initial concentration of liquid-phase P, and C_t (mg L^{-1}) represents the blank corrected concentration of P at time t. W (g) depicts the amount of dried sediment (g), and V is volume of P solution (L).

Sorption kinetics was described respectively by pseudo-first-order and pseudo-second-order models as follows [19,20]:

$$Q_t = Q_e\left(1 - e^{-K_1 t}\right) \tag{3}$$

$$\frac{t}{Q_t} = \frac{1}{K_2 Q_e^2} + \frac{t}{Q_e} \tag{4}$$

Table 1
Physicochemical properties (mean value ± standard deviation) of sediments and water (N = 7) in Liangshui River

	TP (mg kg^{-1})	TN (mg kg^{-1})	OM (%)	Water content (%)	pH
Raw sediment	1845.3 ± 167.5	3892.1 ± 273.2	10.67 ± 1.23	75.22 ± 12.32	8.37 ± 0.71
	TP (mg L^{-1})	TN (mg L^{-1})	NH_3-N (mg L^{-1})	DO (mg L^{-1})	pH
Water	0.89 ± 0.08	9.31 ± 1.05	6.48 ± 0.55	0.4 ± 0.12	8.18 ± 0.66

Table 2
Physicochemical properties (mean value ± standard deviation) of four sediment materials

	Surface area (m^2 g^{-1})	Al_2O_3 (%)	Fe_2O_3 (%)	SiO_2 (%)	Na_2O (%)
PS	9.61 ± 0.74	22.32 ± 2.52	5.90 ± 0.87	60.12 ± 5.18	1.35 ± 0.09
PS-Na	15.87 ± 0.95	20.81 ± 1.95	6.06 ± 0.67	60.43 ± 4.20	1.42 ± 0.07
PS-N	25.01 ± 1.23	21.62 ± 1.77	3.36 ± 0.23	67.81 ± 5.08	2.71 ± 0.12
PS-NNa	30.07 ± 1.82	21.40 ± 2.32	3.07 ± 0.24	67.32 ± 5.12	2.29 ± 0.18

where Q_e represents uptake amount (mg L^{-1}) of P adsorbed at equilibrium time (mg g^{-1}). K_1 (h^{-1}) refers to first-order kinetic rate constant, and K_2 corresponds to sorption rate constant of pseudo-second-order kinetic model (g mg^{-1} min^{-1}).

Sorption isotherms were described by Langmuir and Freundlich models, and equations of isotherm parameters are as follows:

$$Q_e = \frac{Q_m K C_e}{1 + K Q_m} \tag{5}$$

$$Q_e = K_f C_e^n \tag{6}$$

where Q_m represents maximum amount of P uptake (mg g^{-1}), C_e refers to P concentration in aqueous phase at equilibrium (mg L^{-1}), and K corresponds to affinity parameter (L mg^{-1}). K_f is sorption coefficient (L g^{-1}), and n depicts a constant utilized to measure sorption intensity or surface heterogeneity [21].

Thermodynamic parameters were analyzed with the following equations [22,23]:

$$K_D = \frac{C_0 - C_e}{C_e} \times \frac{V}{m} \tag{7}$$

$$\Delta G° = -RT \ln\ln\left(K_D\right) \tag{8}$$

$$\ln\left(K_D\right) = -\frac{\Delta H°}{RT} + \frac{\Delta S°}{R} \tag{9}$$

where $\Delta G°$ (KJ mol^{-1}) represents change in Gibb's free energy; $\Delta S°$ (KJ mol^{-1} K^{-1}) refers to change in entropy; $\Delta H°$ (KJ mol^{-1} K^{-1}) corresponds to change in enthalpy; K_D is an equilibrium constant (dimensionless); R (8.314 J mol^{-1} K^{-1}) is gas constant; $T(K)$ stands for absolute temperature; m(g) represents mass of gravel sand.

3. Results and discussion

3.1. Characterization of sediment materials

3.1.1. Morphological analysis

Fig. 2 shows SEM images of surface structure and morphology of raw and modified sediment materials. Raw sediments feature a smooth and flat surface, as shown in Fig. 1a. Modified sediment materials contain a large number of pores and feature a stratified structure (Figs. 1b, c, d). Large amounts of pores and stratified structure appeared in modified sediments, especially in PS-NNa, which presented an increased surface area (Table 2) that makes surface structure more conductive to sorption [24].

3.1.2. FTIR analysis

Fig. 3 shows FTIR spectra of four sediment materials. The peak at 3425 cm^{-1} in four sediment samples corresponds to stretching vibration of hydroxyl [25]. A strong peak at 1384 cm^{-1} only existed in PS-N. This phenomenon can be

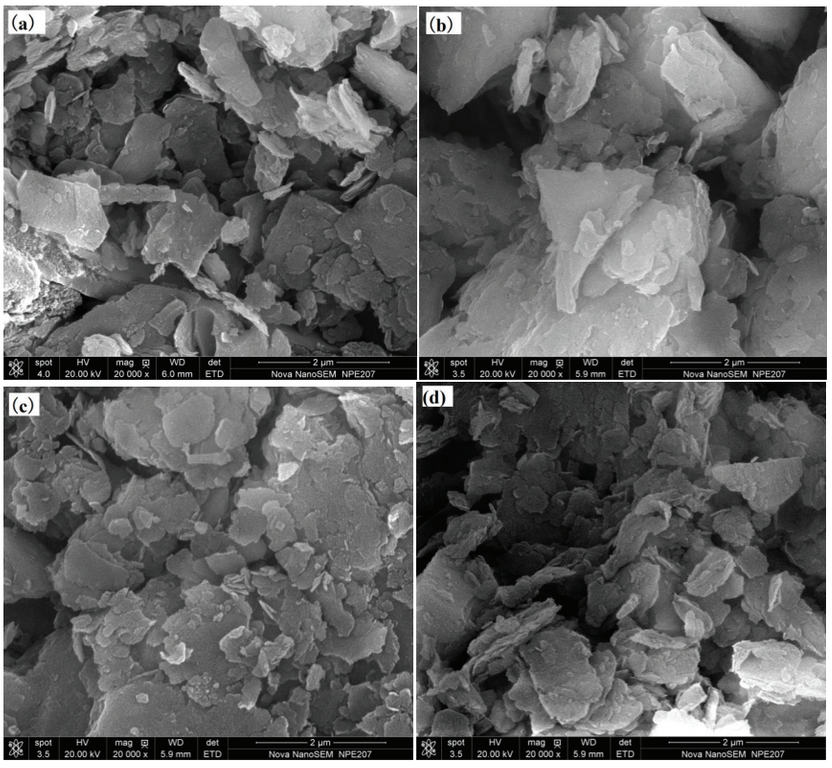

Fig. 2. SEM images of four sediment samples; (a), (b), (c), and (d) represent PS, PS-Na, PS-N, and PS-NNa, respectively.

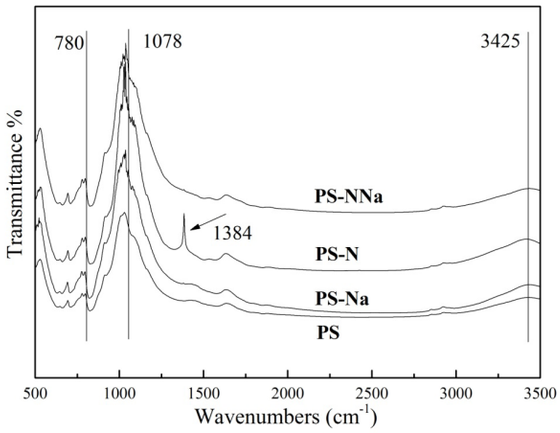

Fig. 3. FTIR spectra of sediment materials.

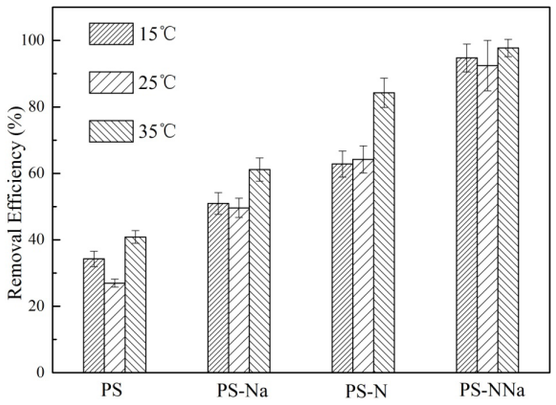

Fig. 4. Effect of temperature on removal of P using four sediment materials.

explained by sediment oxidation, which caused changes in functional groups; stretching vibration of Si–O–Si, Si–O, and O–H also possibly occurred in PS-N [26]. In three modified sediment materials (i.e., PS-Na, PS-N, and PS-NNa), the peak at 1078 cm^{-1} is assigned to metallic bonding or hydrogen bonding caused by oxidation and Na^+ doping [22,24]. Therefore, modified sediment materials possibly supply new active sites for sorption.

3.2. Evaluation of P removal efficiency under different temperatures

Fig. 4 shows the effects of temperature on P removal efficiency. Results showed that PS-NNa exhibited the highest P removal efficiency (>90%), followed by PS-N (62.8%–84.3%) and PS-Na (49.6%–61.1%). Influence of temperature on P removal efficiency differed slightly at 15 and 25°C, whereas P removal efficiency of modified materials increased rapidly as temperature increased to 35°C. Modified materials exhibited higher P removal efficiency than raw sediment samples. This phenomenon resulted from enhancement of sediment surface activities in sediment samples oxidized by HNO_3; loading with a layer of higher active substances changed physicochemical properties (Table 2) of sediment surface of PS-Na. Then, P sorption capacity of modified sediment materials improved dramatically. Temperature significantly affected P sorption capability. Removal efficiency of modified materials generally increased when temperature was increased from 15°C to 35°C. Increase in temperature within limits intensified molecular motion, accelerated diffusion rate, and enhanced probability of H_2PO_4–crashing the surface of modified sediments [27]. On the other hand, more high-energy $H_2PO_4^-$ were adsorbed in sediment surface, improving sorption effect [28].

3.3. P sorption kinetics

Fig. 5 provides experimental results corresponding to P sorption on four sediment materials under study (Q_t vs. t). Results indicate initially rapid P sorption on four sediment materials; P sorption increased rapidly during the first few minutes (0 min to 10 min) but slowed down after initial uptake. P sorption of four samples reached equilibrium at 40 min. Rapid original sorption can be due to physical sorption mechanisms, such as electrostatic interactions, which led to adhesion of P to material surface at the initial stage. Decreasing sorption rate thereafter can be interpreted as caused by lig and exchange [29].

Table 3 presents rate constants and parameters of pseudo-first-order and pseudo-second-order models; these values were derived from nonlinear regression. Correlation coefficients (R^2) demonstrated that pseudo-second-order models better fit data ($R^2 > 0.93$) than pseudo-first-order models. In solutions with an initial P concentration of 10 mg L^{-1}, PS-NNa showed the highest P uptake capacity (up to 0.48 mg g^{-1}) among the four sediment materials, and all sediment materials yielded higher values of Q_e at 35°C than under other temperatures. Table 3 exhibits changes insorption rate constant K_2. Sorption rate constants of the four modified materials followed the order: PS-NNa > PS-Na≈PS-N > PS. High ambient temperature indicated high K_2 values. Physicochemical properties, morphology, and FTIR analysis indicated that oxide contents (Table 2), specific surface area (Table 2), crystal structure (Fig. 2), and surface functional groups (Fig. 3) of modified materials changed due to oxidation and Nadoping, resulting in improved P sorption. Na possibly possessed stronger complexing ability with surface activity site of material particles and reacted more easily with oxygen-containing functional groups when temperature was increased. Therefore, modified material PS-NNa featured high K_2 value at high-temperature conditions.

3.4. Fitting of sorption isotherms

In this study, isotherm data were fitted by Langmuir and Freundlich models [Eqs. (5) and (6)]. Fig. 6 and Table 4 show results of P sorption isotherm experiments. According to correlation coefficients (R^2), the Langmuir model can describe P sorption isotherm better than Freundlich model. Langmuir sorption affinity parameter (K) and maximum sorption capacity (Q_e) of four materials exhibited continuous increase with increasing temperature and reached the high-

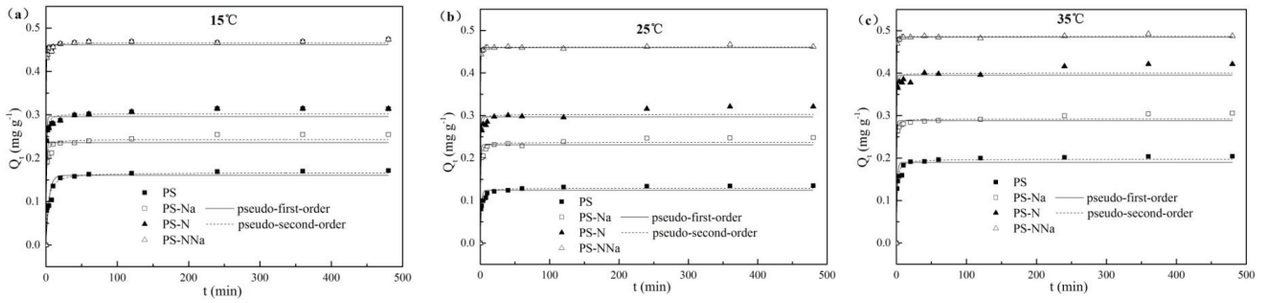

Fig. 5. Sorption kinetics of P on four sediment materials at various temperatures: (a) 25°C; (b) 35°C; (c) 45°C.

Table 3
Fitting kinetics and mechanism parameters of P sorption on four sediment materials according to pseudo-first-order and pseudo-second-order models at three different temperatures

Temperature	Samples	Pseudo-first-order model			Pseudo-second-order model		
		Q_e (mg g^{-1})	K_1 (min^{-1})	R^2	Q_e (mg g^{-1})	K_2 (g mg^{-1} min^{-1})	R^2
15°C	PS	0.161 ± 0.007	0.246 ± 0.055	0.8555	0.167 ± 0.005	2.663 ± 0.588	0.9362
	PS-Na	0.236 ± 0.005	1.331 ± 0.263	0.9334	0.243 ± 0.004	10.242 ± 2.122	0.9733
	PS-N	0.296 ± 0.005	1.522 ± 0.242	0.9631	0.303 ± 0.004	10.696 ± 1.886	0.9854
	PS-NNa	0.462 ± 0.003	2.637 ± 0.316	0.9939	0.466 ± 0.002	22.595 ± 3.663	0.9978
25°C	PS	0.124 ± 0.004	0.719 ± 0.134	0.9104	0.130 ± 0.002	8.783 ± 1.327	0.9749
	PS-Na	0.231 ± 0.004	1.771 ± 0.364	0.9523	0.237 ± 0.003	15.961 ± 3.741	0.9788
	PS-N	0.297 ± 0.005	2.174 ± 0.522	0.9584	0.303 ± 0.005	17.610 ± 5.586	0.9757
	PS-NNa	0.460 ± 0.001	3.359 ± 0.254	0.9991	0.461 ± 0.001	53.011 ± 7.471	0.9996
35°C	PS	0.190 ± 0.005	0.874 ± 0.162	0.9189	0.197 ± 0.003	7.181 ± 1.159	0.9745
	PS-Na	0.288 ± 0.004	2.312 ± 0.433	0.9782	0.292 ± 0.003	22.836 ± 5.726	0.9890
	PS-N	0.395 ± 0.006	2.606 ± 0.648	0.9733	0.400 ± 0.005	19.956 ± 7.325	0.9825
	PS-NNa	0.485 ± 0.001	3.415 ± 0.257	0.9992	0.487 ± 0.001	53.139 ± 7.477	0.9997

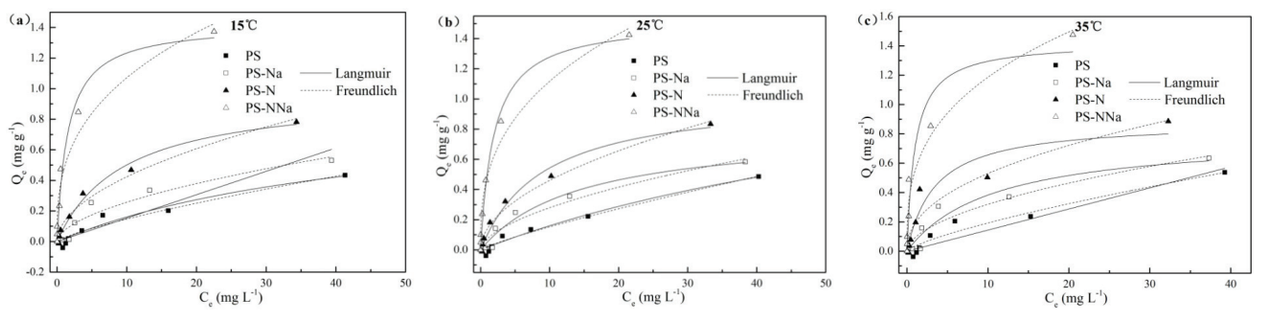

Fig. 6. Sorption isotherms of P on four sediments at different temperatures.

est values of 0.987 L mg^{-1} and 1.43 mg g^{-1} (PS-NNa) at 35°C, respectively. Adsorbed P amount of four materials at equilibrium increased with increasing P concentration in solution. This phenomenon indicates that equilibrium concentration of solutions is closely related to surface coverage density of adsorbent, and higher equilibrium concentration resulted in expanded surface coverage of adsorbents. Thence, at high equilibrium concentrations, a large number of active sites on surface of material particles were occupied by the adsorbate; driving force of sorption decreased and finally reached saturation state [30]. Equilibrium sorption capacity of four materials increased with increasing temperature, which accelerated diffusion rate and led to adsorption of additional high-energy P in particle surface. The value of n obtained by the Freundlich model can reflect strength of sorption capacity of materials; smaller n implies easier adsorption of adsorbate in materials [31]. Overall modified sediment materials promoted P sorption, especially PS-NNa,which showed higher K_f value and adsorption distribution coefficient and capacity when combined with P [32].

Table 4
Langmuir and Freundlich isotherm parameters of P sorption on four sediment materials

Temperature	Samples	Langmuir			Freundlich		
		Q_m (mg g^{-1})	K (L mg^{-1})	R^2	n	K_f (L g^{-1})	R^2
15°C	PS	0.717 ± 0.117	0.021 ± 0.015	0.9325	0.770 ± 0.136	0.025 ± 0.011	0.9240
	PS-Na	0.833 ± 0.087	0.023 ± 0.033	0.9423	0.561 ± 0.100	0.071 ± 0.230	0.9082
	PS-N	0.980 ± 0.076	0.104 ± 0.021	0.9847	0.520 ± 0.054	0.128 ± 0.022	0.9676
	PS-NNa	1.225 ± 0.094	0.642 ± 0.098	0.9758	0.353 ± 0.045	0.475 ± 0.059	0.9505
25°C	PS	0.742 ± 0.096	0.012 ± 0.009	0.9655	0.837 ± 0.107	0.022 ± 0.008	0.9623
	PS-Na	0.839 ± 0.101	0.070 ± 0.023	0.9612	0.573 ± 0.088	0.075 ± 0.021	0.9320
	PS-N	1.033 ± 0.089	0.111 ± 0.025	0.9809	0.512 ± 0.048	0.141 ± 0.021	0.9744
	PS-NNa	1.255 ± 0.081	0.515 ± 0.092	0.9858	0.358 ± 0.035	0.490 ± 0.046	0.9735
35°C	PS	0.754 ± 0.072	0.096 ± 0.032	0.9871	0.750 ± 0.128	0.034 ± 0.015	0.9273
	PS-Na	0.908 ± 0.148	0.089 ± 0.043	0.9158	0.538 ± 0.102	0.093 ± 0.031	0.8946
	PS-N	1.315 ± 0.038	0.287 ± 0.085	0.8910	0.445 ± 0.082	0.190 ± 0.048	0.8947
	PS-NNa	1.426 ± 0.167	0.987 ± 0.123	0.9200	0.334 ± 0.039	0.550 ± 0.058	0.9611

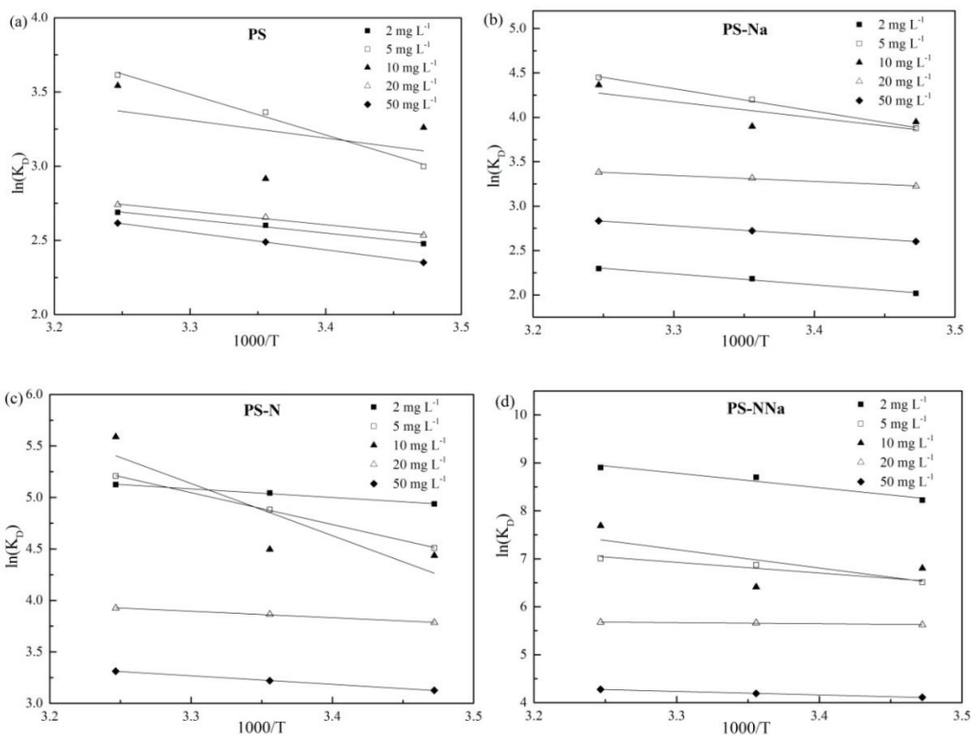

Fig. 7. Thermodynamic analysis for P sorption onto PS, PS-Na, PS-N, and PS-NNa.

The fitting results according the isotherm sorption indicated that the modified sediment had the high P sorption capacity, and the sediment from Liangshui River had the potential of resource utilization. Compared with other materials, ceramic sand (0.51 mg g^{-1}), zeolite (0.46 mg g^{-1}), and shale (0.65 mg g^{-1}) [33,34], PS-NNa had the higher P sorption capacity (1.43 mg g^{-1}). Our previous studied also indicated that the modified lake sediment and gravel had the P sorption capacity of 1.57 and 1.20 mg g^{-1} [17,35], and the samples from Liangshui River had the similar P sorption capacity. Therefore, from the resource utilization of sediment and P removal point of view, the modified sediment might be potential sorbents for P removal and resource utilization.

3.5. Thermodynamic parameters

The plot of ln K_D vs. 1000/T according to Eq. (9) shows a straight line with slope $\Delta H^0/R$ and intercept $\Delta S^0/R$ (Fig. 7). Thermodynamic parameters were calculated and

Table 5
Thermodynamic parameters for P sorption on PS, PS-Na, PS-N, and PS-NNa

C_0 (mg L^{-1})	PS					PS-Na				
	ΔH° (KJ mol^{-1})	ΔS° (KJ mol^{-1} K^{-1})	ΔG° (KJ mol^{-1})			ΔH° (KJ mol^{-1})	ΔS° (KJ mol^{-1} K^{-1})	ΔG° (KJ mol^{-1})		
			15°C	25°C	35°C			25°C	35°C	45°C
2	7.82	0.05	−5.93	−6.44	−6.88	10.31	0.05	−4.83	−5.41	−5.88
5	22.78	0.10	−7.18	−8.33	−9.26	21.12	0.11	−9.28	−10.40	−11.39
10	9.98	0.06	−7.81	−7.22	−9.07	15.13	0.08	−9.46	−9.65	−11.18
20	7.57	0.05	−6.07	−6.58	−7.02	5.65	0.05	−7.72	−8.21	−8.65
50	9.81	0.05	−5.63	−6.17	−6.70	8.56	0.05	−6.23	−6.74	−7.26
C_0 (mg L^{-1})	PS-N					PS-NNa				
	ΔH° (KJ mol^{-1})	ΔS° (KJ mol^{-1} K^{-1})	ΔG° (KJ mol^{-1})			ΔH° (KJ mol^{-1})	ΔS° (KJ mol^{-1} K^{-1})	ΔG° (KJ mol^{-1})		
			25°C	35°C	45°C			25°C	35°C	45°C
2	6.98	0.07	−11.82	−12.49	−13.12	25.19	0.16	−19.69	−21.56	−22.80
5	25.77	0.13	−10.80	−12.10	−13.34	18.46	0.12	−15.59	−17.03	−17.95
10	42.07	0.18	−10.62	−11.14	−14.31	31.84	0.16	−16.29	−15.88	−19.69
20	5.15	0.05	−9.06	−9.58	−10.05	1.91	0.05	−13.47	−14.03	−14.54
50	6.90	0.05	−7.48	−7.98	−8.48	6.15	0.06	−9.84	−10.39	−10.95

are shown in Table 5. Change in Gibbs energy, ΔG°, can be calculated by Eq. (8). Four sediment materials yielded positive values of ΔH° for P sorption; this result indicates that sorption was endothermic in nature [36]. Similar to ΔH°, ΔS° of the four sediments also yielded positive values. Molecular movement at sediment interface became more chaotic after sorption caused by water molecule desorption on material surface; more chaotic movement was also observed from material surface to solution [17]. Negative values of ΔG° (Table 5) indicate that P sorption was spontaneous [37]. Results in Table 5 illustrate that ΔG° values decreased with increasing temperature; this result indicates higher sorption impetus at higher temperature [38]. Sediment materials of PS-N and PS-NNa exhibited smaller ΔG° values than the other two sediment materials, confirming higher sorption capacities of PS-N and PS-NNa. ΔG° values increased as initial P concentration increased, indicating that desorption occurred more easily than sorption at the same temperature [39].

4. Conclusion

Solutions must be obtained for problems of excessive P and utilization of sediment resources in malodorous rivers. P removal efficiency using modified sediment from malodorous river was evaluated, and P sorption mechanism was studied through kinetics, equilibrium, and thermodynamic experiments. Results of this study showed that oxidation-Na-doped materials featured the highest P removal efficiency. Sediment sorption rate followed the pseudo-second-order model, and high temperatures favored P uptake. Overall data describing sorption isotherms were better fitted by Langmuir models. Maximum P sorption capacities followed the order PS-NNa > PS-N > PS-Na > PS, and PS-NNa yielded the highest value of 1.43 mg g^{-1}. According to calculation of thermodynamic parameters for sediment materials, sorption was feasible or spontaneous (ΔG < 0), randomly entropy-driven (ΔS > 0), and endothermic (ΔH > 0). This study provides a new method for utilization of sediment resources and theoretical foundation for control of P in malodorous rivers.

Acknowledgement

This work was supported by Beijing Natural Science Foundation (8174080), Project founded by China Postdoctoral Science Foundation (2017M610968), and the Major Science and Technology Program for Water Pollution Control and Treatment (No. 2017ZX07206).

References

[1] J. Zhu, Y. He, J. Wang, Z. Qiao, Y. Wang, Z. Li, M. Huang, Impact of aeration disturbances on endogenous phosphorus fractions and their algae growth potential from malodorous river sediment, Environ. Sci. Pollut. Res. Int., 24 (2017) 8062–8070.
[2] Y.R. Zhu, F.C. Wu, Z.Q. He, J.Y. Guo, X.X. Qu, F.Z. Xie, J.P. Giesy, H.Q. Liao, F. Guo, Characterization of organic phosphorus in lake sediments by sequential fractionation and enzymatic hydrolysis, Environ. Sci. Technol., 47 (2013) 7679–7687.
[3] X.Q. Tang, M. Wu, X.C. Dai, P.H. Chaia, Phosphorus storage dynamics and adsorption characteristics for sediment from a drinking water source reservoir and its relation with sediment compositions, Ecol. Eng., 64 (2014) 276–284.
[4] W. Huang, Y. Lu, J.H. Li, Z. Zheng, J.B. Zhang, X. Jiang, Effect of ionic strength on phosphorus sorption in different sediments from a eutrophic plateau lake, RSC Adv., 5 (2015) 79607–79615.
[5] G. Martins, L. Peixoto, S. Teodorescu, P. Parpot, R. Nogueira, A.G. Brito, Impact of an external electron acceptor on phosphorus mobility between water and sediments, Biores. Technol., 151 (2014) 419–423.
[6] Y. He, Y.X. Chen, Y.F. Zhang, M.S. Huang, Role of aerated turbulence in the fate of endogenous nitrogen from malodorous river sediments, Environ. Eng. Sci., 30 (2013) 11–16.

[7] B. Liu, R.M. Han, W.L. Wang, H. Yao, F. Zhou, Oxygen microprofiles within the sediment-water interface studied by optode and its implication for aeration of polluted urban rivers, Environ. Sci. Pollut. Res., 24 (2017) 9481–9494.
[8] J. Ma, W. Liu, Effectiveness and mechanism of potassium ferrate (VI) preoxidation for algae removal by coagulation, Water Res., 36 (2002) 871–878.
[9] M. Romantschuk, I. Sarand, T. Petänen, R. Peltola, M. Jonssonvihanne, Means to improve the effect of in situ bioremediation of contaminated soil: an overview of novel approaches, Environ. Pollut., 107 (2000) 179–185.
[10] F. Maillard, O. Girardclos, M. Assad, C. Zappelini, J.M.P. Mena, L. Yung, C. Guyeux, S. Chretien, G. Bigham, C. Cosio, M. Chalot, Dendrochemical assessment of mercury releases from a pond and dredged-sediment landfill impacted by a chlor-alkali plant, Environ. Res., 148 (2016) 122–126.
[11] Z.D. Gu, H.J. Wang, B. Chen, H. Xu, Z.S. Wu, Laboratory solidification experiment on electro-osmotic dehydration and tamping densification of sediment sludge in water plants, J. Food Agr. Environ., 10 (2012) 1149–1152.
[12] D.L. Zhang, H.N. Kong, D.Y. Wu, S.B. He, Z.B. Hu, L.W. Dai, Impact of pyrolysis treatment on heavy metals in sediment, Soil Sediment Conta., 18 (2009) 754–765.
[13] J. Lin, Y. Zhan, Z. Zhu, Evaluation of sediment capping with active barrier systems (ABS) using calcite/zeolite mixtures to simultaneously manage phosphorus and ammonium release, Sci. Total Environ., 409 (2011) 638–646.
[14] K. Sakadecan, H.J. Babvor, Phosphate adsorption characteristics of soils, slags, and zeolites to be used as substrates in constructed wetland systems, Water Res., 32 (1998) 393–399.
[15] J. Bouzid, Z. Elouear, M. Ksibi, A. Feki, A. Montiel, A study on removal characteristics of copper from aqueous solution by sewage sludge and pomace ashes, J. Hazard. Mater., 152 (2008) 838–845.
[16] G.M. Ayoub, B. Koopman, N. Pandya, Iron and aluminum hydroxy (oxide) coated filter media for low-concentration phosphorus removal, Water Environ. Res., 73 (2001) 478–485.
[17] W. Huang, L. Zhang, J. Gao, J. Li, J. Zhang, Z. Zheng, Removal of dissolved inorganic phosphorus with modified gravel sand: kinetics, equilibrium, and thermodynamic studies, Desalin. Water Treat., 57 (2016) 3074–3084.
[18] H. Huo, H. Lin, Y. Dong, H. Cheng, H. Wang, L. Cao, Ammonia-nitrogen and phosphates sorption from simulated reclaimed waters by modified clinoptilolite, J. Hazard. Mater., 229–230 (2012) 292–297.
[19] P. Janoš, P. Michálek, L. Turek, Sorption of ionic dyes onto untreated low-rank coal – oxihumolite: A kinetic study, Dyes Pigments, 74 (2007) 363–370.
[20] Y. Onganer, C. Temur, Adsorption dynamics of Fe(III) from aqueous solutions onto activated carbon, J. Colloid Interf. Sci., 205 (1998) 241–244.
[21] C. Sairam Sundaram, N. Viswanathan, S. Meenakshi, Uptake of fluoride by nano-hydroxyapatite/chitosan, a bioinorganic composite, Biores. Technol., 99 (2008) 8226–8230.
[22] S.Y. Yoon, C.G. Lee, J.A. Park, J.H. Kim, S.B. Kim, S.H. Lee, J.W. Choi, Kinetic, equilibrium and thermodynamic studies for phosphate adsorption to magnetic iron oxide nanoparticles, Chem. Eng. Jo., 236 (2014) 341–347.
[23] C. Namasivayam, D. Sangeetha, Equilibrium and kinetic studies of adsorption of phosphate onto $ZnCl_2$ activated coir pith carbon, J. Colloid. Interf. Sci., 280 (2004) 359–365.
[24] F. Ying, Y. Shui-li, Characterization and phosphorus removal of poly-silicic-ferric coagulant, Desalination, 247 (2009) 442–455.
[25] Z.F. Wang, M. Shi, J.H. Li, L. Zhou, Z.W. Wang, Z. Zheng, Sorption of dissolved inorganic and organic phosphorus compounds onto iron-doped ceramic sand, Ecolog. Eng., 58 (2013) 286–295.
[26] Y.P. Guo, D.A. Rockstraw, Physical and chemical properties of carbons synthesized from xylan, cellulose, and Kraft lignin by H_3PO_4 activation, Carbon, 44 (2006) 1464–1475.
[27] B. Kostura, H. Kulveitova, J. Lesko, Blast furnace slags as sorbents of phosphate from water solutions, Water Res., 39 (2005) 1795–1802.
[28] H. Ye, F. Chen, Y. Sheng, G. Sheng, J. Fu, Adsorption of phosphate from aqueous solution onto modified palygorskites, Sep. Purif. Technol., 50 (2006) 283–290.
[29] C. Ding, X. Yang, W. Liu, Y. Chang, C. Shang, Removal of natural organic matter using surfactant modified iron oxide-coated sand, J. Hazard. Mater., 174 (2010) 567–572.
[30] J. Liu, L. Wan, L. Zhang, Q. Zhou, Effect of pH, ionic strength, and temperature on the phosphate adsorption onto lanthanum-doped activated carbon fiber, J. Colloid Interf. Sci., 364 (2011) 490–496.
[31] A. Fouladi Tajar, T. Kaghazchi, M. Soleimani, Adsorption of cadmium from aqueous solutions on sulfurized activated carbon prepared from nut shells, J. Hazard. Mater., 165 (2009) 1159–1164.
[32] P.S. Kumar, S. Ramalingam, C. Senthamarai, M. Niranjanaa, P. Vijayalakshmi, Adsorption of dye from aqueous solution by cashew nut shell: Studies on equilibrium isotherm, kinetics and thermodynamics of interactions, Desalination, 261 (2010) 52–60.
[33] A. Drizo, C.A. Frost, J. Grace, K.A. Smith, Physico-chemical screening of phosphate-removing substrates for use in constructed wetland systems, Water Res., 33 (1999) 3595–3602.
[34] C.A. Arias, M. Del Bubba, H. Brix, Phosphorus removal by sands for use as media in subsurface flow constructed reed beds, Water Res., 35 (2001) 1159–1168.
[35] W. Huang, B.H. Zheng, X. Jiang, Effect of ionic strength on phosphorus removal with modified sediments in lake: kinetics and equilibrium studies, Int. J. Electrochem. SC, 11 (2016) 9972–9986.
[36] G. Alagumuthu, M. Rajan, Equilibrium and kinetics of adsorption of fluoride onto zirconium impregnated cashew nut shell carbon, Chem. Eng. J., 158 (2010) 451–457.
[37] L. Huang, L. Fu, C. Jin, G. Gielen, X. Lin, H. Wang, Y. Zhang, Effect of temperature on phosphorus sorption to sediments from shallow eutrophic lakes, Ecolog. Eng., 37 (2011) 1515–1522.
[38] K. Li, Z. Zheng, X. Huang, G. Zhao, J. Feng, J. Zhang, Equilibrium, kinetic and thermodynamic studies on the adsorption of 2-nitroaniline onto activated carbon prepared from cotton stalk fibre, J. Hazard. Mater., 166 (2009) 213–220.
[39] D. Kim, Adsorption characteristics of Fe(III) and Fe(III)–NTA complex on granular activated carbon, J. Hazard. Mater., 106 (2004) 67–84.